Broadband Tracking of Characteristic Modes

Jianbin Zhu, Weiwen Li, and Liangcai Zhang

Department of Electronic Engineering, Xiamen University, Xiamen 361005, P. R. China
807408442@qq.com, wwl@xmu.edu.cn, 13194086664@163.com

Abstract ─ Effective mode sorting is the key to achieving characteristic mode (CM) analysis for open conductors. However, mode ordering just according to the eigenvalue magnitude may cause the mode crossing in the operating band. Mode tracking must be performed to obtain the correct mode ordering. Currently, mode tracking based on eigenvector correlation is usually only applicable to narrowband cases due to the large interval between the sampling frequency point and the first frequency. In this paper, the correlation calculation is directly performed between two adjacent frequencies, and the first frequency is not used as the anchor point. Due to the improvement of the eigenvector correlation, the broadband mode tracking is realized. Some numerical examples are used to verify the effectiveness of this algorithm.

Index Terms ─ Characteristic mode theory, broadband, eigenvector correlation, mode tracking.

I. INTRODUCTION

The characteristic mode (CM) theory is a useful tool that allows us to analyze antenna radiating properties using a systematic approach [1-4]. After the impedance matrix of the open conductor has been obtained by Galerkin method of moment (MoM), a generalized eigenvalue equation can be constructed using the real and imaginary part of the matrix. The eigenvectors physically correspond to the characteristic current wavemodes, which form a weighted orthogonal set over the conductor surface [5].

The modes can be sorted according to the eigenvalue magnitude at each frequency point. However, since the eigenvalues are sensitive to frequency variations, the ordering of modes at higher frequencies may differ from that obtained at lower frequencies [6]. Similarly, for geometrically symmetric conductors with degenerate modes, the mode ordering based on tracking eigenvalues alone cannot also work well [7]. For these reasons, it is more common to perform mode tracking based on eigenvector correlation [8, 9]. In that case, the first frequency sample is selected as the reference frequency, and the vector correlation algorithm is used to determine the mode ordering at each subsequent frequency [10].

Since the starting frequency is used as the reference point, the interval between the subsequent frequency samples and the reference frequency will increase as the frequency increases. When the operating frequency band is wide enough, the last frequency point is far away from the first one, and the mode swapping problem is prone to occur, especially for higher order modes [10]. We refer to this mode tracking algorithm based on initial frequency correlation as the original algorithm, which can be implemented by parallel operations.

To eliminate the mode swapping of wideband mode tracking, we propose to perform eigenvector pairing and correlation calculation for all directly adjacent two frequencies. In this method, the mode ordering of subsequent frequencies cannot be performed until mode sorting at the previous frequency is completed. That is to say, the mode correlation is performed by serial operation. However, mode tracking can be implemented over a wide band due to the large correlation of adjacent frequency modes. So we called it the broadband mode tracking, or the improved algorithm.

II. MODE SORTING

According to CM theory, the current distribution of the conductor surface can be expressed as the superposition of characteristic current vector J_n:

$$J = \sum_n \alpha_n J_n, \qquad (1)$$

where α_n is the complex weighting coefficient of the nth mode. The characteristic current mode J_n is determined by the generalized eigenvalue equation [5]:

$$X J_n = \lambda_n R J_n. \qquad (2)$$

The impedance matrix $Z = R + jX$ of the open conductor obtained by Galerkin MoM is a symmetric matrix. λ_n is the eigenvalue of the nth mode and is the function of frequency. Since the eigenvalue equation depends only on the impedance matrix, in the physical sense, the current wavemode eigenvectors depend only on the shape and size of the conductor structure and is not affected by the excitation source [11-14]. The eigenvalues are also determined only by the conductor structure. Moreover, since X and R are real symmetric matrices, and R also is a positive definite matrix, the eigenvalues obtained by solving (2) are real numbers. It is necessary to sort the modes within the observed frequency range to

use CM theory. At each discrete frequency sample, the modes can be sorted according to the eigenvalue, the modal significance (MS), or the characteristic angle [3]. The most intuitive method is based on the eigenvalue magnitude, which is arranged in ascending order at each frequency.

However, since the eigenvalues change rapidly with frequency, mode swapping is apt to occur. Due to the orthogonality of the characteristic modes and their slow variation with frequency, the eigenvector correlation is generally used for mode tracking to reduce the mode crossing. The correlation coefficient r between vectors A and B can be calculated using the Pearson correlation formula [8, 9]:

$$r(A,B) = \frac{1}{M-1} \frac{\sum\limits_{i=1}^{M}(A_i - \bar{A})(B_i - \bar{B})}{\sqrt{\sum\limits_{i=1}^{M}(A_i - \bar{A})^2 \sum\limits_{i=1}^{M}(B_i - \bar{B})^2}}, \quad (3)$$

where (A_i, B_i) is the vector element pair to be compared, and $\bar{A}$ and $\bar{B}$ are the average of the real vector A and B, respectively. M is the dimension of the vectors A and B, that is, the number of vector elements. Correlation value r ranges between -1 and 1. The closer the absolute value of r is to 1, the higher the correlation between the two vectors. When (3) is used in the mode tracking algorithm, A is the characteristic mode obtained by calculating (2) at a certain frequency, and B is the CM at other frequencies to be paired with A.

If the correlation calculation involves all vector pairs between two frequency points, it is computationally expensive and time-consuming. However, for electrically small and intermediate size conductor bodies, the actual surface current or total radiation field is determined by only the first few characteristic modes. Therefore, we can also reduce the number of vectors used for correlation calculations. For example, to determine the first five modes, only the first 40 eigenvectors are selected for correlation calculation. Nonetheless, the total number of eigenvectors for each frequency is equal to the dimension of the conductor impedance matrix, which is determined by the structure mesh fineness. In fact, since external excitation is not required, the eigenvector results depend only on the calculation of the impedance matrix. Therefore, the accuracy of CM analysis depends mainly on the meshing density, which also determines the calculation amount of the impedance matrix and the number of eigenvalues. When higher order modes are needed in CM analysis, the high mesh density with the mesh element side length of $\lambda/30$ (λ is the wavelength in free space) is suggested. Usually, to ensure the CM analysis accuracy, the mesh fineness with side length of $\lambda/15$ is enough [10].

III. MODE TRACKING BASED ON ORIGINAL ALGORITHM

In CM theory, the mode order is defined according to the ascending eigenvalues at the first frequency. In the original algorithm, the mode order of the subsequent frequency samples is determined by calculating the correlation between the first frequency eigenvectors and those for subsequent frequencies. This algorithm process can be illustrated as shown in Fig. 1.
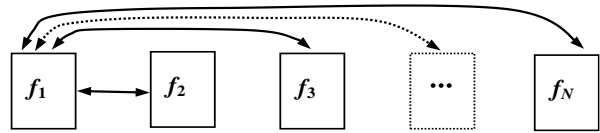

Fig. 1. Illustration of parallel correlation computing process in the original algorithm.

Using this algorithm, the mode curve can be obtained quickly, and mode crossing does not occur in a relatively narrow frequency band, especially for regular conductor structures [10]. However, for broadband situations, mode swapping may happen due to the large frequency span, especially for cases with structure irregularities. To illustrate these issues exemplarily, the algorithm is used to analyze the first five modes of rectangular and butterfly conductor plates in the range from 1 GHz to 5 GHz.

First, the 100 mm × 40 mm rectangular conductor plate is meshed into 512 triangular Rao-Wilton-Glisson (RWG) elements with side length of about $\lambda/15$, as shown in Fig. 2. Thus, we have a total of 744 triangular edges, which also corresponds to the dimension of the impedance matrix. Using (2), we can obtain 744 eigenvalues at each frequency point. The frequency step is 0.2 GHz, that is, the eigenvalue calculation is performed on 21 frequency samples. At each frequency point, the first 40 eigenvectors are selected in ascending order of eigenvalues.
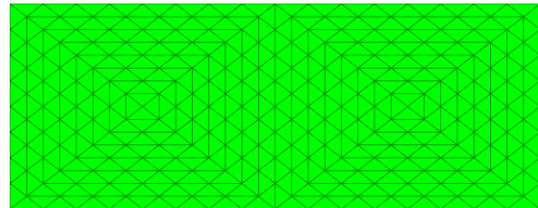

Fig. 2. Meshing of the 100 mm × 40 mm rectangular conductor plate.

Then, the correlation coefficients of the 40 eigenvector pairs between the first frequency and each

subsequent frequency are calculated, and the mode matching is performed using the correlation amplitude according to the mode order of the first frequency. This process is also called the mode arbitration.

The obtained mode tracking curve is shown in Fig. 3. Due to large frequency range, the mode 5 exhibits swapping at around 3.6 GHz. It indicates that this mode arbitration method can only achieve mode tracking in a narrower frequency band. However, this algorithm can implement fast mode tracking because, in addition to parallel operations, the eigenvector number for correlation calculations is limited. Of course, this algorithm can also be implemented by serial operation. In that case, mode sorting for this example takes 12.68 s. In this paper, all the calculations are performed on an Intel Core i7-6700HQ (2.6 GHz) machine with Windows 7 Professional 64 bit and 8 GB of RAM.
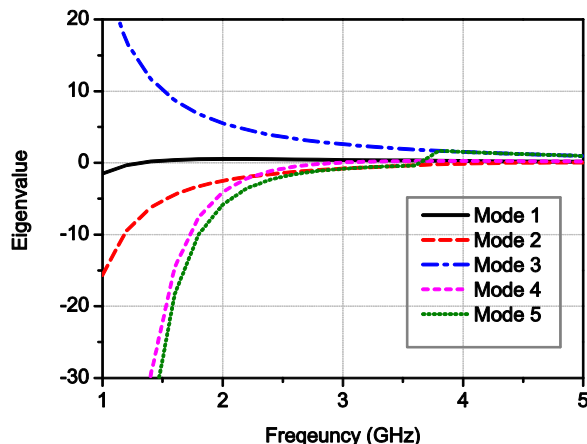

Fig. 3. Mode curves of 100 mm × 40 mm rectangular conductor plate using the original algorithm.

When there are electric field concentration regions in the conductor structure, mode swapping is easily generated, and the frequency range of mode tracking may be further reduced. For this case, tracking of the first five modes for the planar butterfly structure is performed in the range of 1.0-3.0 GHz. The frequency step is also 0.2 GHz.

To form the butterfly structure plate, as shown in Fig. 4, two isosceles triangles having the base length of 200 mm and the waist length of 141 mm are cut out from a 200 mm × 200 mm rectangular conductor plate. Strong electric fields can be concentrated on the thin waist of the butterfly structure. The butterfly plate is discretely meshed using the triangular RWG elements with the side length of approximately $\lambda/15$. Then the number of triangle elements is 720, corresponding to a total of 1025 triangular edges, also shown in Fig. 4.

Using the original tracking algorithm, the resulted mode curve for the butterfly conductor is shown in Fig.

5. It can be seen that mode swapping occurs in the mode 5 curve around 2.2 GHz. This shows that as the conductor structure becomes more complex, the mode tracking bandwidth using the original algorithm will be further reduced. By serial operation, the time for completing the mode tracking of this example is 20.84 s.
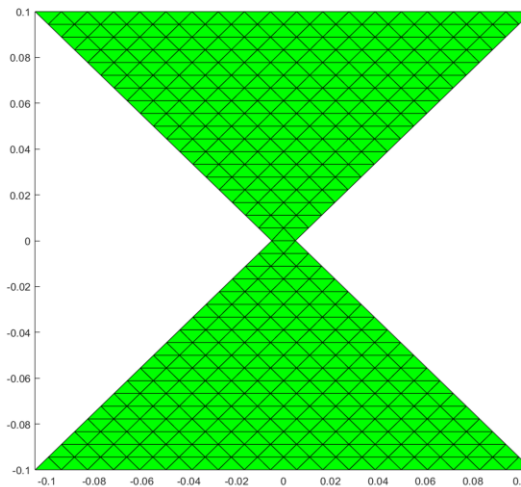

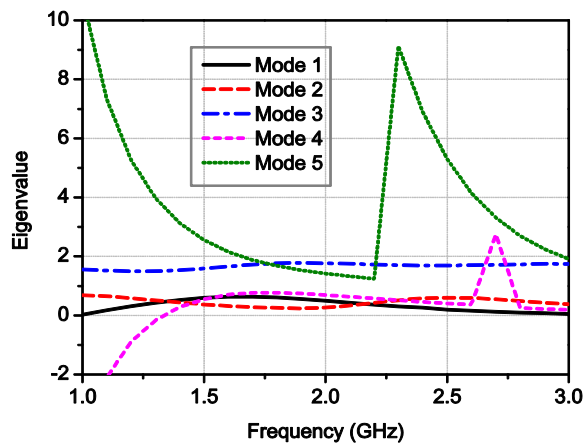Fig. 4. Meshing model of butterfly conductor plate (unit: m).

Fig. 5. Mode curves of the butterfly conductor plate based on the original algorithm.

IV. IMPLEMENTATION OF BROADBAND MODE TRACKING

Since the bandwidth of mode tracking is limited by the eigenvector correlation between two frequencies and the span between the first frequency and the last one may be large, the improved algorithm for mode arbitration based on direct adjacent two frequency points is proposed. Specifically, the eigenvectors of the first frequency match those of the second frequency, and then the eigenvectors of the second frequency match those of

the third frequency, and so on. By this way, the first five modes at all frequency samples are determined.

It can be seen that the modes of the current frequency cannot be determined until the modes of the previous frequency are sorted. This tracking process is a serial operation and its calculation speed may be reduced compared to the original parallel algorithm. However, the mode crossing can be eliminated in wide band owing to the fixed frequency interval. Figure 6 shows the mode arbitration process of this broadband mode tracking algorithm.
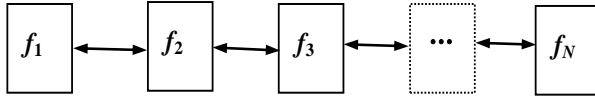

Fig. 6. Mode arbitration illustration of the broadband tracking algorithm.

As an example, the first five modes of the 100 mm × 40 mm rectangular plate are tracked using the mode arbitration method with two directly adjacent frequencies. The obtained first five modes are shown in Fig. 7. We can observe that mode 5 does not exhibit mode swapping. Here, the same mesh density, the same frequency range, and the same frequency step as the case shown in Fig. 3 is used. The mode sorting time using this algorithm is 12.79 s. It indicates that this algorithm can also implement fast mode tracking. In fact, in this example, the first five modes can be tracked in the frequency range of 1.0-10.0 GHz without the mode swapping.
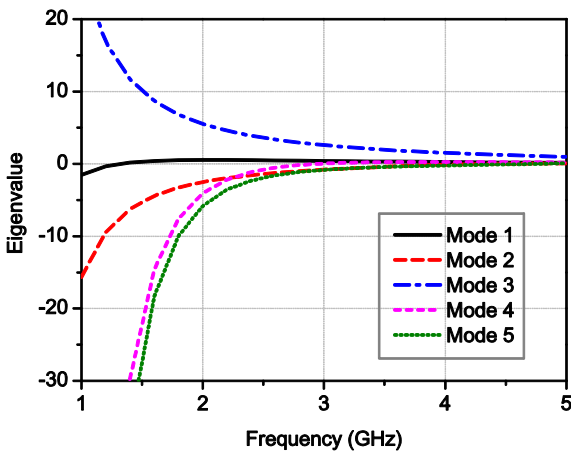

Fig. 7. First five modes of the 100 mm × 40 mm conductor plate based on the wideband algorithm.

Similarly, the butterfly structure shown in Fig. 4 is also subjected to mode tracking using the present method. When the other conditions remain completely unchanged, the resulting mode curve is shown in Fig. 8.

We can see the mode crossing is effectively suppressed in the range from 1 GHz to 3 GHz. In this case, the tracking time of the first five modes is 21.14 s. Using this algorithm, we can also verify that the first five modes can be tracked in the 1.0-4.7 GHz frequency range without the mode crossing. All of those demonstrate the effectiveness of the wideband algorithm.
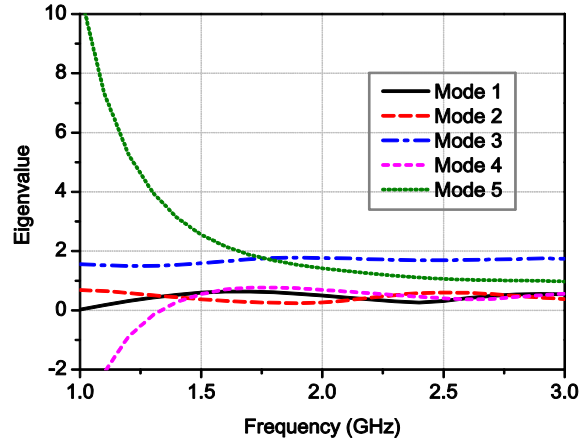

Fig. 8. Mode curves of butterfly structure obtained by using the wideband algorithm.

V. ANALYSIS AND DISCUSSION

A. Cause of mode swapping

For the original algorithm, there are two possible reasons for the occurrence of mode crossing. One is the insufficient calculation accuracy due to the low mesh density, and the other is low eigenvector correlation due to the excessive frequency spacing. The mode swapping shown in Fig. 3 and Fig. 5 is due to the excessive spacing between frequencies f_1 and f_n, rather than due to insufficient mesh density.

To further verify this point of view, the mesh density is doubled to the butterfly structure. Using the original algorithm, we still obtain the mode curves as shown in Fig. 5, which indicates that the mode crossing is not caused by meshing.

B. Number of correlation eigenvector pairs

Although only the first five modes are determined in the numerical examples, we have to calculate the correlation between 40×40 eigenvector pairs. Therefore, the amount of correlation calculation is still large. In fact, the calculation amount can be further reduced according to the number of modes to be sorted, for example, the first five modes.

First, the first five modes of the first frequency are determined with ascending order eigenvalues, and the correlation coefficients between these five modes and the first 40 modes of the second frequency are solved. Then, the first five modes of the second frequency are ordered and used to calculate their correlation with the first 40

modes of the third frequency. By this way, the first five modes for all the frequency points are determined. Thus, the eigenvector pair number of the correlation calculation between the two frequency points is reduced from 40×40 of the wideband algorithm to 5×40.

C. Parallel operation of wideband algorithm

The wideband algorithm is performed completely in series. However, since the time required for mode sorting is small, we can first calculate the correlation of all adjacent frequency modes in parallel, and then sort modes according to the correlation using serial operation. On the other hand, since there are no first five modes that have been determined beforehand, the correlation calculation is performed on all 40×40 eigenvector pairs of the two adjacent frequencies. Thus, the parallel operation of the wideband algorithm contradicts the number of the correlation eigenvector pairs.

D. Reference frequency and frequency step

Intuitively, the intermediate frequency can also be used as the reference point to improve the working bandwidth of the mode tracking algorithm. However, as can be seen, the eigenvalues of the starting reference frequency are greater than those of the subsequent frequencies. If the intermediate frequency is selected as the reference point, the eigenvalue decreases as the frequency decreases in the first half of the frequency band. In this case, the mode curve loses its physical meaning.

On the other hand, it is of course possible to reduce the computation amount of the algorithm by increasing the frequency step. However, if the frequency interval is too large, the vector correlation between two frequency points is weakened and the mode crossing is apt to occur. Therefore, the frequency step should be a compromise between computational speed and mode crossing control.

VI. CONCLUSION

Considering the need of broadband high-precision mode tracking, the serial operation between direct adjacent frequencies is used in mode correlation calculation. The numerical results show that this algorithm can reliably improve the bandwidth of mode tracking and effectively control the mode crossing. Since correlation calculations are performed using a limited number of eigenvectors, less time is required to complete wideband mode tracking.

The mode tracking bandwidth implemented by this algorithm is sufficient in practical applications. In fact, characteristic mode analysis should not be used in excessive bandwidth, otherwise misleading problems may occur.

REFERENCES

[1] K. K. Kishor and S. V. Hum, "Multiport multiband chassis-mode antenna design using characteristic modes," *IEEE Antenna Wirel. Propag. Lett.*, vol. 16, pp. 609-612, 2017.

[2] R. Martens and D. Manteuffel, "Systematic design method of a mobile multiple antenna system using the theory of characteristic modes," *IET Microwave Antennas Propagat.*, vol. 8, no. 12, pp. 887-893, Sept. 2014.

[3] Y. Chen and C. F. Wang, "Characteristic-mode-based improvement of circularly polarized U-slot and E-shaped patch antennas," *IEEE Antenna Wirel. Propag. Lett.*, vol. 11, pp. 1474-1477, 2012.

[4] M. Cabedo-Fabres, E. Antonino-Daviu, A. Valero-Nogueira, and M. F. Bataller, "The theory of characteristic modes revisited: A contribution to the design of antennas for modern applications," *IEEE Antenna Propag. Mag.*, vol. 49, no. 5, pp. 52-68, Oct. 2007.

[5] R. Harrington and J. Mautz, "Theory of characteristic modes for conducting bodies," *IEEE Trans. Antennas Propag.*, vol. 19, no. 5, pp. 622-628, Sept. 1971.

[6] M. Capek, P. Hazdra, P. Hamouz, and J. Eichler, "A method for tracking characteristic numbers and vectors," *Prog. Electromagn. Res.*, vol. 33, pp. 115-134, 2011.

[7] E. Safin and D. Manteuffel, "Advanced eigenvalue tracking of characteristic modes," *IEEE Trans. Antennas Propag.*, vol. 64, no. 7, pp. 2628-2636, July 2016.

[8] D. J. Ludick, J. V. Tonder, and U. Jakobus, "A hybrid tracking algorithm for characteristic mode analysis," in *Proc. Int. Conf. Electromagn. Adv. Appl.*, Palm Beach, FL, pp. 455-458, Aug. 2014.

[9] D. J. Ludick, U. Jakobus, and M. Vogel, "A tracking algorithm for the eigenvectors calculated with characteristic mode analysis," in *Proc. 8th European Conf. Antennas and Propagation (EuCAP)*, The Hague, Netherlands, pp. 569-572, Apr. 2014.

[10] W. Li, J. Zhu, B. Xu, and Z. Zeng, "Fast implementation of characteristic mode tracking," *IET Microwave Antennas Propagat.*, vol. 12, no. 14, pp. 2179-2183, Nov. 2018.

[11] Z. T. Miers and B. K. Lau, "Computational analysis and verifications of characteristic modes in real materials," *IEEE Trans. Antennas Propag.*, vol. 64, no. 7, pp. 2595-2607, July 2016.

[12] Y. Chen, "Alternative surface integral equation-based characteristic mode analysis of dielectric resonator antennas," *IET Microwave Antennas Propagat.*, vol. 10, no. 2, pp. 193-201, Jan. 2016.

[13] Q. He, Z. Gong, H. Ke, and L. Guan, "A double modal parameter tracking method to characteristic modes analysis," *ACES Journal*, vol. 32, no. 12, pp. 1069-1076, Dec. 2017.

[14] A. Araghi and G. Dadashzadeh, "Detail-oriented design of a dual-mode antenna with orthogonal radiation patterns utilizing theory of characteristic modes," *ACES Journal*, vol. 28, no. 10, pp. 952-959, Oct. 2013.